International Journal of Engineering, Science and Mathematics
Vol. 6 Issue 8, December 2017,
ISSN: 2320-0294 Impact Factor: 6.238
Journal Homepage: **http://www.ijesm.co.in, Email: ijesmj@gmail.com**
Double-Blind Peer Reviewed Refereed Open Access International Journal - Included in the International Serial Directories Indexed & Listed at: Ulrich's Periodicals Directory ©, U.S.A., Open J-Gage as well as in Cabell's Directories of Publishing Opportunities, U.S.A

Heat Transfer of Saturated Nanofluid Sandwiched between Permeable fluids

J.C. Umavathi*[1], K. Hemavathi[1] and G. Janardhana Reddy[2]
[1]Department of Mathematics, Gulbarga University, Kalaburgi-585 106, Karnataka, India.
[2]Department of Mathematics, Central University of Karnataka, Kalaburagi- 585 311, Karnataka, India.

Abstract

The objective of this study is to understand the convective heat transfer of water-based nanofluid flowing through a vertical duct. The duct is filled with nanofluid saturated with porous medium sandwiched between permeable fluid. The two vertical walls of the enclosure are kept at constant temperature. The flow in the porous material is defined by Darcy equation. The Boussinesq approximation is invoked so that the effect of density variation is combined with the buoyancy forces. Separate solutions are matched at the interface using suitable matching conditions. Continuity of velocity, continuity of shear stress, continuity of temperature and continuity of heat flux are assumed at the interface. The equations of momentum and energy are coupled and nonlinear. Approximate analytical solutions are obtained using regular perturbation method. Results for a wide range of governing parameters such as Grashof number, Brinkman number, porous parameter, and solid volume fraction are plotted on the flow fields. It is found that the presence of porous matrix and solid volume fraction suppress the velocity and temperature fields where as Grashof number and Brinkman number promotes the flow. Numerical values for the skin friction and the Nusselt number at the left and right walls are also evaluated and are depicted in tabular form.

Keywords : Nanofluids, Porous media, Mixed convection, Vertical duct.

1. Introduction

Nanoparticle colloids have particular physical properties that make them useful for a wide range of applications including paints and coatings, ceramics, drug delivery and food industries [1-3]. Colloids composed of ultrafine nanoparticles (w100 nm or smaller) are called nanofluids. Growing attention has been recently paid to nanofluids because of their enhancement in heat transfer [4-6]. This desirable characteristic opens numerous applications of nanofluids as super-coolant in nuclear reactors, car engines, radiators, computers, X-rays and many other industrial products. Nanofluids are called super-coolant because they can absorb heat more than any traditional fluids, so they can reduce the size of system and increase its performance [3,7]. Oxide ceramics (Al_2o_3, Cuo); nitride ceramics (AlN, SiN); carbide ceramics (SiC, TiC); metals (Ag, Al, Au, Cu, Fe); semiconductors (Sio_2, Tio_2); single, double, or multi wall carbon nanotubes $(SWCNT, DWCNT, MWCNT)$; and composite materials such as nanoparticle core-polymer shell composites are certain materials which are used to produce nanoparticles and are dispersed in a host liquid to make the nanofluid. Water is used as a traditional host liquid due to its high thermal conductivity, abundance, low cost, and friendliness to the environment [7].

Depending on shape, size, and thermal properties of the solid nanoparticles, the thermal conductivity can be increased by about 40% with low concentration (1%–5% by volume) of solid nanoparticles in the mixture [8-12]. The nanofluid is stable, it introduces very little pressure drop, and it can pass through nanochannels (for instance see Zhou [13]). The word "nanofluid" was coined by Choi [14]. Xuan and Li [15] pointed out that at higher nanoparticle volume fractions, the viscosity increases sharply, which suppresses heat transfer enhancement in the nanofluid. Therefore, it is important to carefully select the proper nanoparticle volume fraction to achieve heat transfer enhancement.

Transport processes through porous media play important roles in numerous practical applications in modern industry, such as the design of building components for energy and environmental systems consideration, control of pollutant spread in groundwater, geothermal energy technology, compact heat exchangers, solar power collectors, food industries, and have wide potential applications in many engineering areas including the chemical, oil and gas recovery, polymer, food processing, pharmaceutical, biochemical engineering, etc. Recent decades have seen a spike in the number of studies (Shenoy [16]) devoted to the study of convective flow through porous media. Good literature reviews on convective flow and applications of nanofluids have been done by Buongiorno [17], Das et al. [18], Kakac and Pramuanjaroenkij [19], Jaluria

et al. [20], Mahian et al.[21], Sakai et al. [22], and many others. It is worth pointing out that Sakai et al. [22] have rigorously derived a macroscopic set of the governing equations for describing heat transfer in nanofluids saturated with porous media using a volume averaging theory, for possible heat transfer applications of metal foams filled with nanofluids as high performance heat exchangers.

Stability analysis of nanofluid saturated with porous medium was investigated by Umavathi and Mohite [23-25] and Umavathi et al. [26]. Umavathi [27] studied the gravity modulation for Rayleigh-Benard convection in a horizontal channel filled with nanofluid saturated with porous medium. Recently Umavathi et al. [28] and Umavathi and Mikhail [29] discussed the stability analysis of double-diffusive convection for the nanofluid saturated with porous medium and for a micropolar nanofluid saturated with porous medium in a horizontal channel. Umavathi and Prathap [30] also worked for stability features using Oldroyd nanofluid. Umavathi and her group [31,32] investigated the heat transfer enhancement of nanofluid filled in a duct for both constant and variable prosperities. A multilayer liquid arrangement provides an improved model for buoyancy-driven convective process in growing high-quality crystals Schwabe [33]. The multilayer problem formulation now contains additional dynamical ingredients such as the interfacial stress and the deformation of the interface shape. Alazmi and Vafai [34] provided different types of interfacial conditions. In this paper the model considered is as given by Vafai and Thiyagaraja [35] which states that there is a continuity of shear stress and heat flux at the interface. Following the model of Vafai and Thiyagaraja [35], Umavathi et al. [36-42] published series of papers on heat and mass transfer of immiscible fluid in various geometries taking into account the mixture of Newtonian and non-Newtonian fluids also.

The above literature review revealed that there is no any work done on mixed convection in a porous open ducts filled with a nanofluid for immiscible fluids. The present study is therefore an attempt to fill this deficiency.

2. Mathematical Formulation

The physical configuration considered in this study is shown in Fig. 1. We consider a steady, laminar mixed convective flow of three immiscible fluids filled in a vertical channel. The X-axis is taken parallel to the channel, while the Y-axis is taken perpendicular to it. The region $-h \le y \le 0$ and $h \le y \le 2h$ is occupied by the porous fluid having density ρ_f, the viscosity μ_f, the thermal conductivity k_f and the thermal expansion coefficient β_f and the region $0 \le y \le h$ is occupied by nano fluid saturated with porous matrix having density ρ_{nf}, the viscosity μ_{nf}, the thermal conductivity k_{nf} and the thermal expansion coefficient β_{nf}. The flow in all the three regions are assumed to be incompressible and fully developed. The thermo physical properties are assumed to be constant except for the density in the buoyancy term in the momentum equation. The fluid rises in the channel driven by buoyancy forces.

The transport properties for both regular and nanofluid are assumed to be constant. The boundary walls of the channel are held at different constant temperatures, i.e., T_{w1} at the left wall and T_{w2} at the right wall with $T_{w1} \ge T_{w2}$. We use the Boussinesq approximation, i.e., the density is constant everywhere except when it is multiplied by gravity. Further we also make the assumptions that, at the two interfaces, there is continuity of velocities, shear stresses, temperatures and heat flux. Applying all the above assumptions the governing equations for the system defined become

Region-I

$$\mu_f \frac{d^2u_1}{dy^2} + (\rho_f g \beta_f)(T_1 - T_{w2}) - \frac{\mu_f}{\kappa} u_1 - \frac{\partial p}{\partial x} = 0 \quad (1)$$

$$k_f \frac{d^2T_1}{dy^2} + \mu_f \left(\frac{du_1}{dy}\right)^2 + \frac{\mu_f}{\kappa} u_1^2 = 0 \quad (2)$$

Region-II

$$\mu_{nf} \frac{d^2u_2}{dy^2} + (\rho_{nf} g \beta_{nf})(T_2 - T_{w2}) - \frac{\mu_{nf}}{\kappa} u_2 - \frac{\partial p}{\partial x} = 0 \quad (3)$$

$$k_{nf} \frac{d^2T1}{dy^2} + \mu_{nf} \left(\frac{du_2}{dy}\right)^2 + \frac{\mu_{nf}}{\kappa} u_2^2 = 0 \quad (4)$$

Region-III

$$\mu_f \frac{d^2u_3}{dy^2} + (\rho_f g \beta_f)(T_3 - T_{w2}) - \frac{\mu_f}{\kappa} u_3 - \frac{\partial p}{\partial x} = 0$$

(5)

$$k_f \frac{d^2T_3}{dy^2} + \mu_f \left(\frac{du_3}{dy}\right)^2 + \frac{\mu_f}{\kappa} u_3^{\,2} = 0$$

(6)

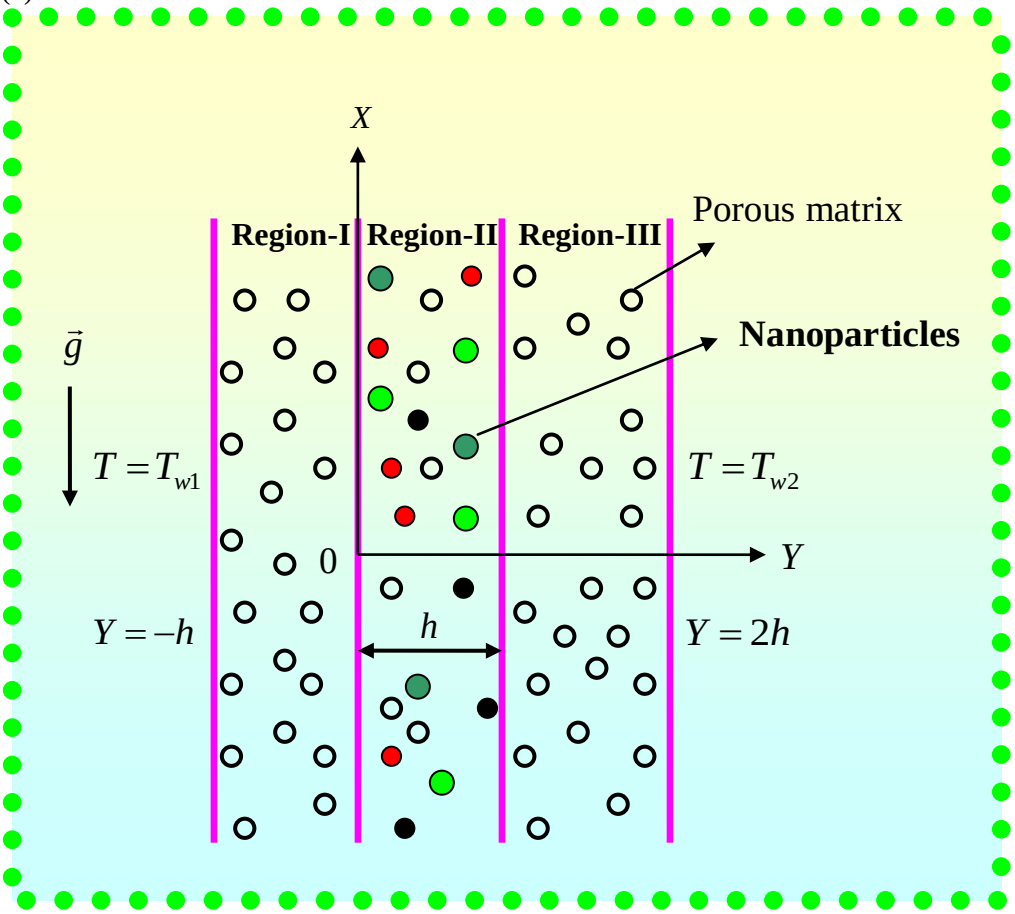

Figure 1. Schematic diagram

To evaluate the constants for the solution of Eqs. (1), (3) and (5), six conditions are required. Two are obtained from the assumption that there is no slip at the walls and the other four conditions are obtained by assuming that the velocities and stresses are equal at the interfaces. Similarly to solve Eqs. (2), (4) and (6), the six boundary conditions needed are, constant wall temperature at the two plates, and the other four conditions are obtained assuming that the temperature and heat flux are equal at the interface. Therefore the boundary and interface conditions for the velocity and temperature are

$$u_1(-h) = 0, \qquad u_1(0) = u_2(0), \qquad \mu_f \frac{du_1(0)}{dy} = \mu_{nf} \frac{du_2(0)}{dy}$$

$$u_2(h) = u_3(h), \qquad \mu_{nf} \frac{du_2(h)}{dy} = \mu_f \frac{du_3(h)}{dy}, \qquad u_3(2h) = 0$$

(7)

$$T_1(-h) = T_{w2}, \qquad T_1(0) = T_2(0), \qquad k_f \frac{dT_1(0)}{dy} = k_{nf} \frac{dT_2(0)}{dy}$$

$$T_2(h) = T_3(h), \qquad k_{nf} \frac{dT_2}{dy}(h) = k_f \frac{dT_3}{dy}(h), \qquad T_3(2h) = T_{w1}$$

(8)

The effective density of nanofluid is given as

$$\rho_{nf} = (1-\phi)\rho_f + \phi\rho_s$$

(9)

where ϕ is the solid volume fraction of the nanoparticles. The thermal diffusivity, heat capacitance and thermal expansion coefficients of the nanofluid respectively are given by

$$\alpha_{nf} = \frac{k_{nf}}{(\rho C_p)_{nf}}$$

(10)

$$(\rho C_p)_{nf} = (1-\phi)(\rho C_p)_f + \phi(\rho C_p)_s$$

(11)

$$(\rho\beta)_{nf} = (1-\phi)(\rho\beta)_f + \phi(\rho\beta)_s$$

(12)

The effective dynamic viscosity of the nanofluid given by Brinkman [43] is

$$\mu_{nf} = \frac{\mu_f}{(1-\phi)^{2.5}}$$

(13)

In Eq (4), K_{nf} is the thermal conductivity of the nanofluid. For spherical nanoparticles, according to Maxwell [44], this can be written as

$$K_{nf} = K_f\left[\frac{K_s + 2K_f - 2\phi(K_f - K_s)}{K_s + 2K_f + \phi(K_f - K_s)}\right]$$

(14)

Here the subscript nf, f and s respectively are the thermo physical properties of the nanofluid, base fluid and the solid nanoparticles. The thermo physical properties of the base fluid and solid nanoparticles are given in Table1.

To transform the Eqs. (1)-(8) into dimensionless form, we introduce the following dimensionless parameters

$$y^* = \frac{y}{h},\quad u_1^* = u_1\left(\frac{\rho_f}{\mu_f}\right)h,\quad u_2^* = u_2\left(\frac{\rho_f}{\mu_f}\right)h,\quad u_3^* = u_3\left(\frac{\rho_f}{\mu_f}\right)h,$$

$$\theta_1 = \frac{T_1 - T_{w2}}{T_{w1} - T_{w2}},\ \theta_2 = \frac{T_2 - T_{w2}}{T_{w1} - T_{w2}},\ \theta_3 = \frac{T_3 - T_{w2}}{T_{w1} - T_{w2}},\ P = -\frac{\rho_f h^3}{{\mu_f}^2}\frac{\partial p}{\partial x},$$

$$Gr = \frac{g\beta_f (T_{w1} - T_{w2})h_3}{{\upsilon_f}^2},\quad Br = \frac{{\mu_f}^3}{{\rho_f}^2 h^2 (T_{w1} - T_{w2})k_f},\ \sigma = \frac{h}{\sqrt{\kappa}}$$

(15)

Substituting the above quantities into Eqs. (1) - (8) , after dropping asterisks we get the following non- dimensionalized equations.

Region-I

$$\frac{d^2u_1}{dy^2} + Gr\theta_1 = 0$$

(16)

$$\frac{d^2\theta_1}{dy^2} + Br\left(\frac{du_1}{dy}\right)^2 = 0$$

(17)

Region-II

$$\frac{d^2u_2}{dy^2} + Gr(1-\phi)^{2.5}\left[(1-\phi) + \frac{\phi(\rho\beta)_s}{(\rho\beta)_f}\right]\theta_2 - \sigma^2 u_2 = 0$$

(18)

$$\frac{d^2\theta_2}{dy^2} + Br\frac{1}{(1-\phi)^{2.5}}\left(\frac{k_s + 2k_f + \phi(k_f - k_s)}{k_s + 2k_f - 2\phi(k_f - k_s)}\right)\left[\left(\frac{du_2}{dy}\right)^2 + \sigma^2{u_2}^2\right] = 0$$

(19)

Region-III

$$\frac{d^2u_3}{dy^2} + Gr\,\theta_3 = 0$$

(20)

$$\frac{d^2\theta_3}{dy^2} + Br\left(\frac{du_3}{dy}\right)^2 = 0$$

(21)

The boundary and interface conditions in the non- dimensional forms become

$$u_1(-1) = 0, \quad u_1(0) = u_2(0), \quad \frac{du_1(0)}{dy} = \frac{\mu_{nf}}{\mu_f}\frac{du_2(0)}{dy}$$

$$u_2(1) = u_3(1), \quad \frac{du_2(1)}{dy} = \frac{\mu_f}{\mu_{nf}}\frac{du_3(1)}{dy}, \quad u_3(2) = 0$$

(22)

$$\theta_1(-1) = 0, \quad \theta_1(0) = \theta_2(0), \quad \frac{d\theta_1(0)}{dy} = \frac{k_{nf}}{k_f}\frac{d\theta_2(0)}{dy}$$

$$\theta_2(1) = \theta_3(1), \quad \frac{d\theta_2(1)}{dy} = \frac{k_f}{k_{nf}}\frac{d\theta_3(1)}{dy}, \quad \theta_3(2) = 1$$

(23)

3. Solutions

The equations which govern the flow along with respective boundary and interface conditions as defined in Eqs. (16) to (21) are ordinary nonlinear coupled equations. Hence closed form solutions are not possible. Therefore we resort to finding approximate analytical solutions. The method opted is regular perturbation method. This is a justifiable method because if one choose Brinkman number as the perturbation parameter, the limitations imposed on the perturbation method is satisfied. It is well known that in many of the practical applications Brinkman number cannot exceed the value one. In view of the above, choosing Brinkman number as the perturbation method, approximate solutions for the velocity and temperature fields can be assumed as

$$u_i(y) = u_{i0}(y) + Bru_{i1}(y) + Br^2u_{i2}(y) + \ldots\ldots\ldots\ldots$$

(24)

$$\theta_i(y) = \theta_{i0}(y) + Br\theta_{i1}(y) + Br^2\theta_{i2}(y) + \ldots\ldots\ldots\ldots$$

(25)

Using Eqs. (24) and (25) into Eqs. (16) to (23) and equating the coefficients of like powers of Brinkman number Br to zero, we obtain the zeroth and first order equations along with their respective boundary and interface conditions as follows.

Zeroth order equations

Region-I

$$\frac{d^2u_{10}}{dy^2} + Gr\,\theta_{10} - \sigma^2u_{10} + P = 0$$

(26)

$$\frac{d^2\theta_{10}}{dy^2} = 0$$

(27)

Region-II

$$\frac{d^2u_{20}}{dy^2} + Gr(1-\phi)^{2.5}\left[(1-\phi) + \frac{\phi(\rho\beta)_s}{(\rho\beta)_f}\right]\theta_{20} - \sigma^2u_{20} + P(1-\phi)^{2.5} = 0$$

(28)

$$\frac{d^2\theta_{20}}{dy^2} = 0$$

(29)

Region-III

$$\frac{d^2u_{30}}{dy^2}+Gr\,\theta_{30}-\sigma^2u_{30}+P=0$$

(30)

$$\frac{d^2\theta_{30}}{dy^2}=0$$

(31)

First order equations

Region-I

$$\frac{d^2u_{11}}{dy^2}+Gr\,\theta_{11}-\sigma^2u_{11}=0$$

(32)

$$\frac{d^2\theta_{11}}{dy^2}+\left(\frac{du_{10}}{dy}\right)^2+\sigma^2{u_{10}}^2=0$$

(33)

Region-II

$$\frac{d^2u_{21}}{dy^2}+Gr\left(1-\phi\right)^{2.5}\left[(1-\phi)+\frac{\phi(\rho\beta)_s}{(\rho\beta)_f}\right]\theta_{21}-\sigma^2u_{21}=0$$

(34)

$$\frac{d^2\theta_{21}}{dy^2}+\frac{1}{(1-\phi)^{2.5}}\left(\frac{ks+2kf+\phi(kf-ks)}{ks+2kf-2\phi(kf-ks)}\right)\left[\left(\frac{du_{20}}{dy}\right)^2+\sigma^2{u_{20}}^2\right]=0$$

(35)

Region-III

$$\frac{d^2u_{31}}{dy^2}+Gr\,\theta_{31}-\sigma^2u_{31}=0$$

(36)

$$\frac{d^2\theta_{31}}{dy^2}+\left(\frac{du_{30}}{dy}\right)^2+\sigma^2{u_{30}}^2=0$$

(37)

Zeroth order boundary and interface conditions are

$$u_{10}(-1)=0,\ u_{10}(0)=u_{20}(0),\ \frac{du_{10}(0)}{dy}=\frac{\mu_{nf}}{\mu_f}\frac{du_{20}(0)}{dy}$$

$$u_{20}(1)=u_{30}(1),\quad \frac{du_{20}(1)}{dy}=\frac{\mu_f}{\mu_{nf}}\frac{du_{30}(1)}{dy},\ u_{30}(2)=0$$

(38)

$$\theta_{10}(-1)=0,\quad \theta_{10}(0)=\theta_{20}(0),\quad \frac{d\theta_{10}(0)}{dy}=\frac{k_{nf}}{k_f}\frac{d\theta_{20}(0)}{dy}$$

$$\theta_{20}(1)=\theta_{30}(1),\quad \frac{d\theta_{20}(1)}{dy}=\frac{k_f}{k_{nf}}\frac{d\theta_{30}(1)}{dy},\quad \theta_{30}(2)=1$$

(39)

First order boundary and interface conditions are

$$u_{11}(-1)=0,\ u_{11}(0)=u_{21}(0),\ \frac{du_{11}(0)}{dy}=\frac{\mu_{nf}}{\mu_f}\frac{du_{21}(0)}{dy}$$

$$u_{21}(1)=u_{31}(1),\ \frac{du_{21}(1)}{dy}=\frac{\mu_f}{\mu_{nf}}\frac{du_{31}(1)}{dy},\ u_{31}(2)=0$$

(40)

$$\theta_{11}(-1)=0,\ \theta_{11}(0)=\theta_{21}(0),\ \frac{d\theta_{11}(0)}{dy}=\frac{k_{nf}}{k_f}\frac{d\theta_{21}(0)}{dy}$$

$$\theta_{21}(1)=\theta_{31}(1),\ \frac{d\theta_{21}(1)}{dy}=\frac{k_f}{k_{nf}}\frac{d\theta_{31}(1)}{dy},\ \theta_{31}(2)=0$$

(41)

The solutions of Eqs. (26) to (41) along with their boundary and interface conditions can be obtained directly by integrating the equations and hence the solutions are not presented.

To understand the physical significance, results for the skin friction and Nusselt number are evaluated numerically and shown in Table 2.

The Nusselt number for the nanofluid in the non-dimensional form is defined as

$$Nu\big]_{y=-1}=-\frac{k_{nf}}{k_f}\left(\frac{d\theta_1}{dy}\right)_{y=-1}\quad\text{and}\quad Nu\big]_{y=2}=-\frac{k_{nf}}{k_f}\left(\frac{d\theta_3}{dy}\right)_{y=2}$$

The skin friction in non-dimensional form is defined as

$$\tau\big]_{y=-1}=\frac{\mu_{nf}}{\mu_f}\left(\frac{du_1}{dy}\right)_{y=-1}\quad\text{and}\quad\tau\big]_{y=2}=\frac{\mu_{nf}}{\mu_f}\left(\frac{du_3}{dy}\right)_{y=2}$$

4. Results and discussion

The convective heat transfer of water-based nanofluid flowing through a vertical duct filled with nanofluid saturated with porous medium sandwiched between permeable fluid is studied analytically. The graphical analysis has been carried out on various pertinent parameters, namely Grashof number Gr, Brinkman number Br, porous parameter σ, solid volume fraction ϕ and are depicted in Figures 2 to 11. The Nusselt number and Skin friction are evaluated and illustrated in the form of Tables.

The effect of Grashof number on the velocity and temperature fields are shown in Figures (2) and (3) considering copper as a nano particle and water as a base fluid. These pictures shows that as Grashof number increases both the velocity and temperature profiles are enhanced in all the three regions. The optimum velocity is observed in the middle of the channel. One can justify this result because $Gr>0$ is buoyancy assisting flow which supports the motion. The Grashof number acts as the driving force in the momentum equation. The velocity and/or velocity gradient increases and therefore the effect of dissipation increases, which results in the enhancement of temperature field also. The effect of Grashof number on the flow field is a classical result for single fluid flowing in a vertical channel. The similar nature is also observed for three immiscible fluid flowing in a vertical channel. The effect of Grashof number on the flow is also the similar result observed by Vajravelu et al. [45]. Vajravelu et al [45] studied the convective transport of nanofluid sandwiched between viscous fluids including the effects of Brownian and thermopheric diffusion. In the present problem Tiwari and Das [46] model is applied to define the nanofluids.

The effect of Brinkman number on the velocity and temperature fields are shown in Figures (4) and (5) respectively for $Gr>0$ and using Copper-water based nanofluids. It is observed that increasing value of Brinkman number increases the velocity and temperature in all the regions. However the effect of enhancement is dominating in region-II when compared to region-I and Region-III. This is also a classical result observed when the channel is filled with one fluid. This is due to the fact that an increase in the Brinkman number results in the increase of dissipation effect which results in the increase of temperature and hence velocity is also enhanced for the increase in buoyancy force in the momentum equation.

The effect of porous parameter on the velocity and temperature fields are shown in Figures (6) and (7) for $Gr>0$ and Copper-water based nanofluid. It is observed that increasing the porous parameter, the velocity and temperature decreases in all the three regions. The flow profiles of both velocity and temperature are parabolic in nature. That is the profile increases initially at the left wall then become parabolic in nature in the middle channel and finally go to zero at the right channel for velocity profiles and one for the temperature profiles at the right channel.

The effect of solid volume fraction is seen in Figures (8) and (9) on the flow field. As the solid volume fraction increases both the velocity and temperature decreases. One can justify this result by saying that as the nanoparticle is added to the pure fluid, the density of the fluid increases and the fluid become denser which results in the decrease of momentum of the fluid in the channel. The effect of solid volume fraction on the flow was the similar result as observed by Umavathi and Shekhar [47] who studied the electrically conducting Jeffery Hamel nanofluid flow in a convergent /divergent channel. The same authors Shekhar and Umavathi [48] also obtained the similar result for the effect of solid volume fraction for the saturated nanofluid flowing in a vertical channel. Using Tiwari and Das model, Umavathi et al. [31,49] also observed the similar results for the effect of solid volume fraction on the flow. In all the above studies the

authors have considered one fluid model. Figure 5 and 6 also suggests that the effect of solid volume fraction is also observed in Region-III which is occupied by a viscous fluid saturated with porous matrix. This is due to the dragging effect of the interfacial conditions.

Flow observation using different nanoparticles using water as a base fluid is shown in Figures 10 and 11. The global view indicates that there is no distinguishable effect on both velocity and temperature fields. However when the graph is enlarged it is seen that for velocity profile the optimal flow is observed using Silver as a nanoparticle and minimal is observed using Silicon oxide(Sio_2) as a nanoparticle and for temperature profiles optimal flow is observed using Silicon oxide as a nanoparticle and minimum is observed using diamond as a nanoparticle. However Umavathi and Shekhar [47] obtained maximum velocity for Silicon oxide nanoparticle and minimal for silver nanoparticle when the channel is filled with only nanofluid. When the nanofluid is filled in a vertical rectangular ducts the optimal velocity is obtained with Silver nanoparticle as observed by Umavathi et al. [49].

The values of Nusselt number and Skin friction is shown in Table 2 for all the governing parameters at both the plates. This table reflects that as the Grashof number, Brinkman number increases the Nusselt number decreases at the left wall , increases at the right wall. Skin friction increases at the left plate and decreases at the right plate where as for solid volume fraction, skin friction increases at the left plate and decreases at the right plate and Nusselt number decreases at the left plate and increases at the right plate. These results are obtained using Copper as nanoparticle and water as a base fluid. The value of Nusselt number and Skin friction using different nanoparticles keeping water as a base fluid shows that Nusselt number is maximum for Silicon oxide nanoparticle and minimum for Silver nanoparticle where as Skin friction is maximum for Silver nanoparticle and minimum for Silicon oxide nanoparticle. However the values tell that there is no influential effects on the Nusselt number and Skin friction for all nanoparticles under study.

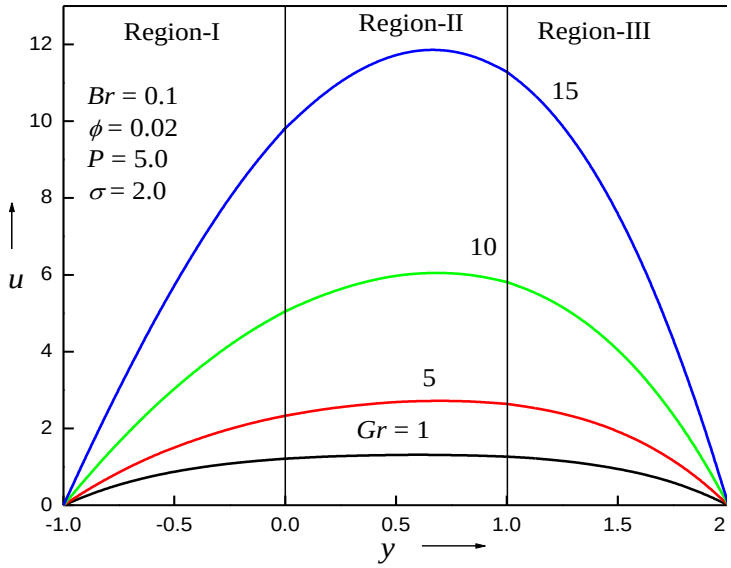

Figure 2. Velocity profiles for different values of Grashoff Number *Gr*.

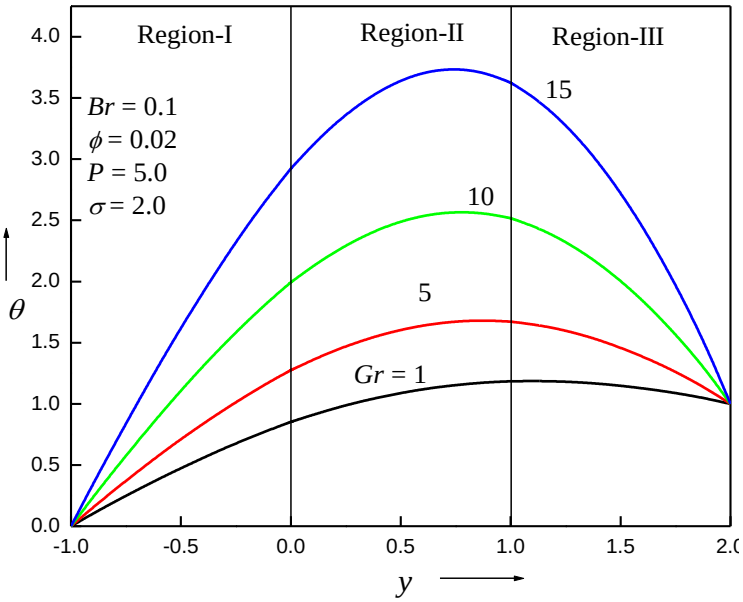

Figure 3. Temperature profiles for different values of Grashof Number *Gr*.

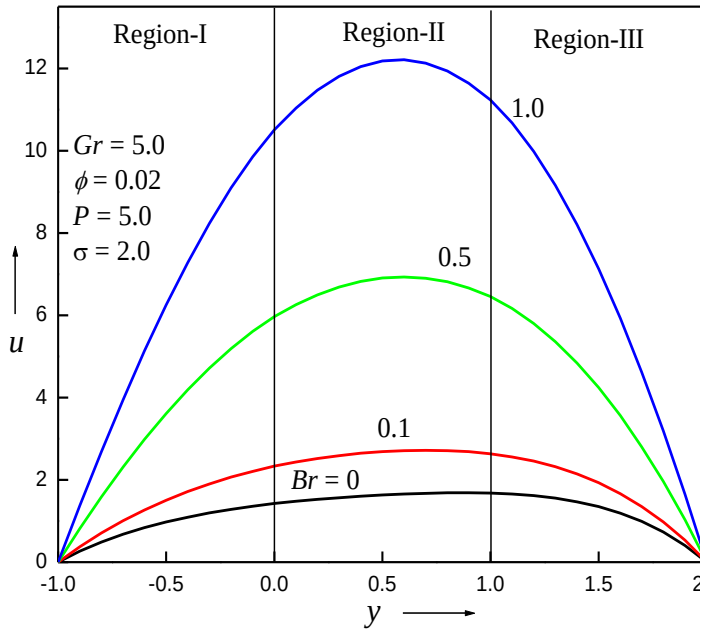

Figure 4. Velocity profiles for different values of Brinkman Number *Br*.

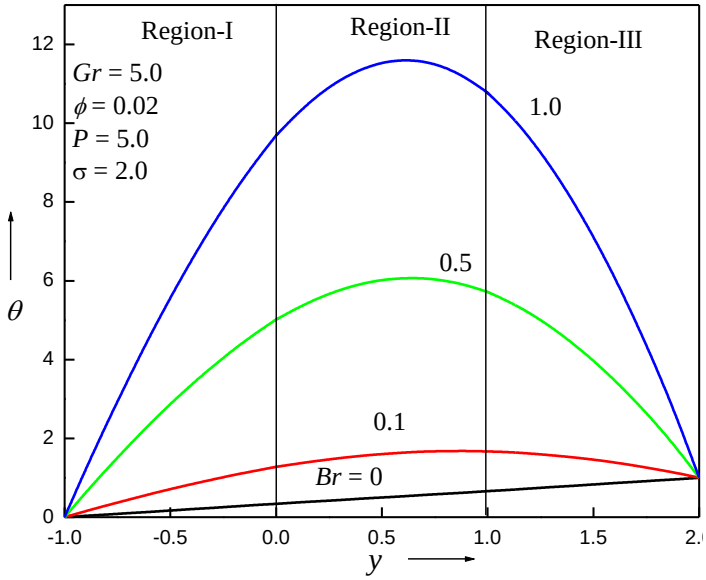

Figure 5. Temperature profiles for different values Brinkman Number Br.

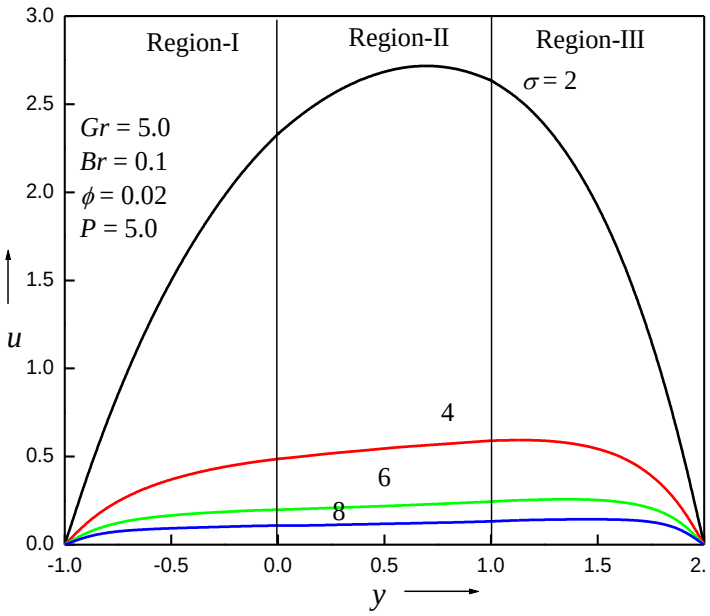

Figure 6. Velocity profiles for different values of porous parameter σ.

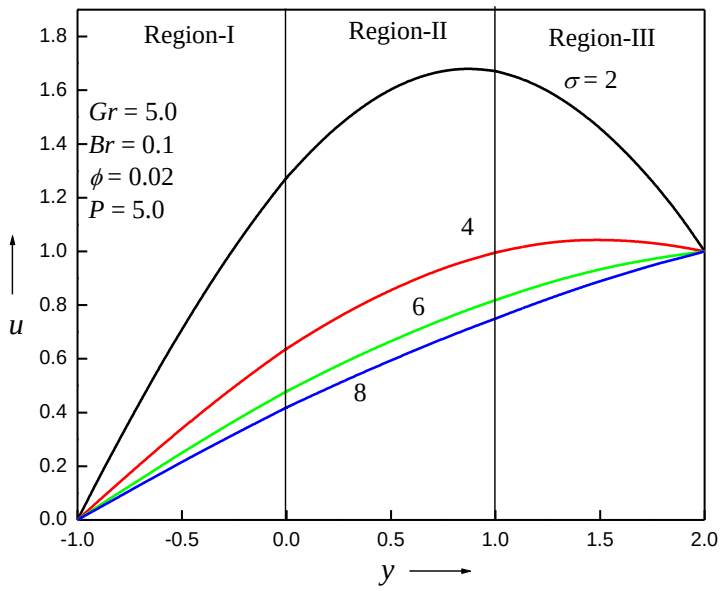

Figure 7. Velocity profiles for different values of porous parameter σ.

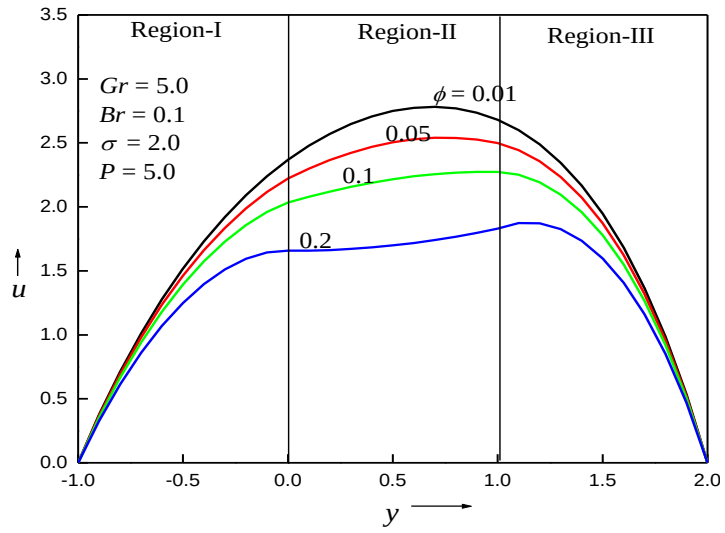

Figure 8. Velocity profiles for different values of solid volume fraction ϕ.

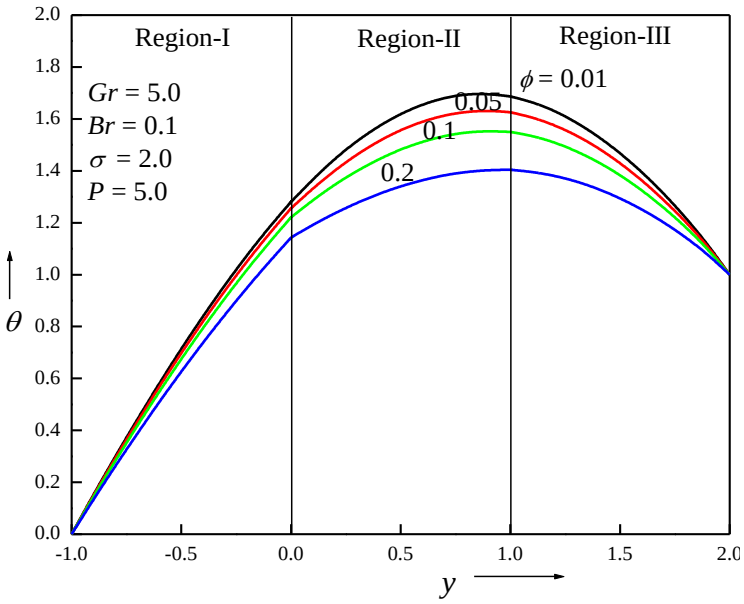

Figure 9. Temperature profiles for different values of solid volume fraction ϕ.

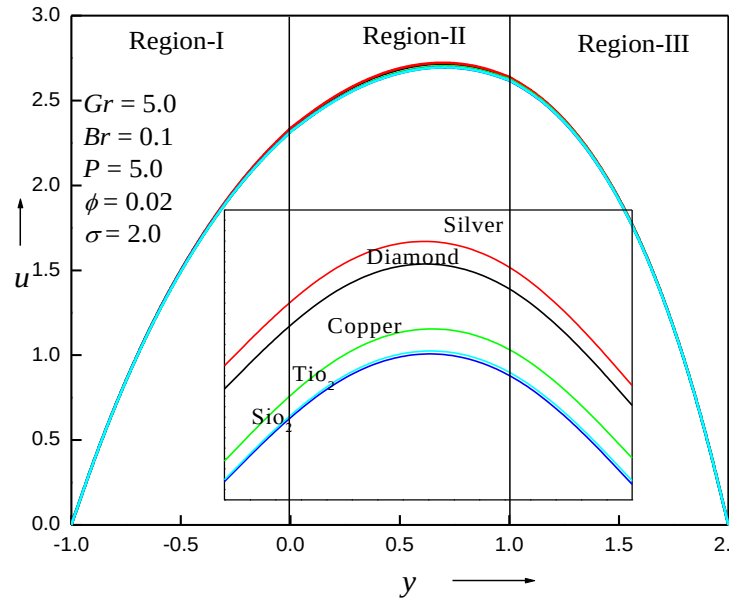

Figure 10. Velocity profiles for different Nanoparticles.

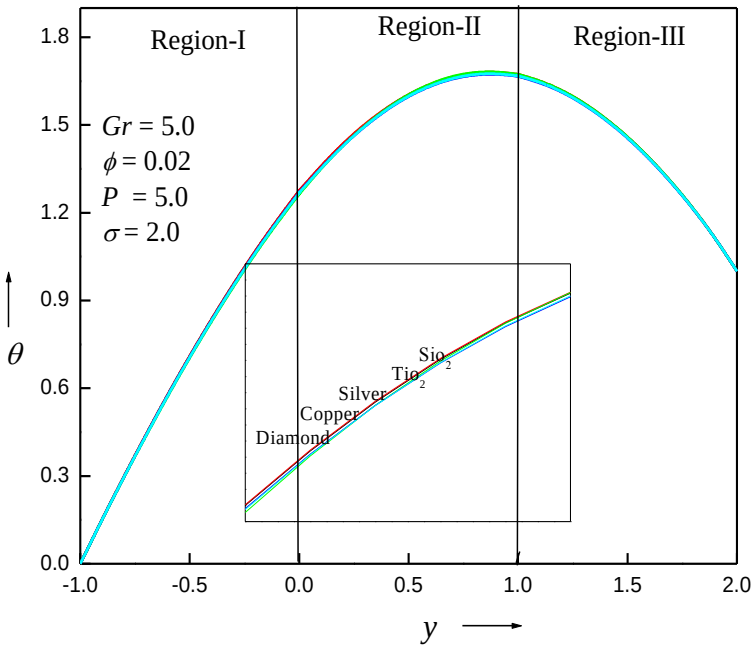

Figure 11. Temperature profiles for different Nanoparticle.

Table 1. Thermo physical properties for pure water and various types of nanoparticles.

Property	Pure water	Ag	Cu	Diamond	SiO2	TiO2
ρ (kg/m^2)	997.1	10500	8933	3510	2200	4250
μ (Nm/s)	0.001	-	-	-	-	-
k (W/mK)	0.613	429	400	1000	1.2	8.5938
C_p (kJ/kgK)	4179	235	385	497.26	703	686.2
β (1/K)	207.10^{-6}	18.10^{-6}	17.10^{-6}	$1.0.10^{-6}$	$5.5.10^{-6}$	$0.17.10^{-6}$

Table 2. Values of Nusselt number and skin friction fixing the values as Gr =5, P =1, Br =0.01 , ϕ =0.02, σ =2 except the varying parameter

	$Nu\rceil_{y=-1}$	$Nu\rceil_{y=2}$	$\tau\rceil_{y=-1}$	$\tau\rceil_{y=2}$
Gr				
1	-0.433621	-0.27889	2.70142	-3.05194
5	-0.479456	-0.192874	3.14581	-4.9103
10	-0.568725	-0.0402591	3.86471	-7.44025

Br 0.01 0.05 0.1	 -0.479456 -0.955083 -1.54962	 -0.192874 0.477827 1.3162	 3.14581 3.6133 4.19765	 -4.9103 -5.43367 -6.08787
ϕ 0.0 0.02 0.05	 -0.443242 -0.479456 -0.537997	 -0.171541 -0.192874 -0.227568	 3.00676 3.14581 3.37144	 -4.69995 -4.9103 -5.25321
Copper Silver SiO_2 Diamond TiO_2	-0.479456 -0.479495 -0.452812 -0.479443 -0.473052	-0.192874 -0.192716 -0.179711 -0.193576 -0.190266	3.14581 3.14656 3.13885 3.14286 3.14183	-4.9103 -4.91117 -4.91153 -4.90684 -4.90783

Table 3. Comparison Table

y	Velocity		Temperature	
	present	Vajravelu et al. [45]	present	Vajravelu et al. [45]
-1	-5.14E-16	-7.59E-16	-2.30E-16	-2.09E-16
-0.8	4.6835	4.6835	1.0418	1.0418
-0.6	8.9641	8.9640	1.7608	1.7608
-0.4	12.6966	12.6966	2.2310	2.2310
-0.2	15.7859	15.7859	2.5206	2.5206
0	18.1731	18.1731	2.6897	2.6897
0.2	19.7438	19.7438	2.7840	2.7840
0.4	20.5982	20.5982	2.8493	2.8493
0.6	20.7236	20.7236	2.9067	2.9067
0.8	20.1091	20.1091	2.9627	2.9627
1	18.7442	18.7442	3.0067	3.0067
1.2	16.5095	16.5095	3.0080	3.0080
1.4	13.4749	13.4749	2.9064	2.9064
1.6	9.6621	9.6621	2.6186	2.6186
1.8	5.1305	5.1305	2.0316	2.0316
2	3.01E-15	5.62E-15	1.0000	1.0000

5. Conclusions.

Analytical studies were carried out to understand the flow nature for the porous nanofluid sandwiched between porous fluid. Tiwari and Das [47] model was used to define the nanofluid. The regular perturbation method was opted to solve the nonlinear coupled equations in all the three regions using Brinkman number as the perturbation parameter. It was concluded that

1. As the Grashof number, Brinkman number and porous parameter increases the flow is promoted in all the three regions where as the solid volume fraction demotes the fluid motion.

2. Optimal flow was observed using Silver as a nanoparticle and minimal flow was observed for Silicon oxide(Sio_2) nanoparticle keeping water as base fluid. However there was no distinguishable influence on the flow using any nanoparticle.
3. The Nusselt number decreases at left wall, Skin friction increases at the left plate and at the right plate skin friction decreases and Nusselt number increases. The solid volume fraction decreases the Nusselt number and increases Skin friction at the left plate but the Nusselt number increases and skin friction decreases at right plate. Optimal Nusselt number and Skin friction was obtained using Silver as a nanoparticle.

Nomenclature

Br	Brinkman number $\left(Br = \frac{{\mu_f}^3}{{\rho_f}^2 h^2 (T_{w1} - T_{w2}) k_f} \right)$
g	Acceleration due to gravity
Gr	Grashof number $\left(Gr = \frac{g\beta_f (T_{w1} - T_{w2}) h_3}{{\upsilon_f}^2} \right)$
h	Channel width
k	Coefficient of thermal conductivity
P	Non dimensional pressure $\left(P = -\frac{\rho_f h^3}{{\mu_f}^2} \frac{\partial p}{\partial x} \right)$
T	Temperature
u	Dimensional velocity
y	Space co-ordinate
τ	Skin friction
λ	Mixed convection parameter

Greek symbols

β	Co-efficient of thermal Expansion
μ	Viscosity
ν	Kinematic viscosity
ϕ	Solid volume fraction
θ	Dimensionless temperature
ρ	Density of clear fluid
σ	porous parameter

Subscripts

nf	Thermo-physical properties of clear and the nanofluids
f	Base fluid
s	Solid nanoparticles
i	Refer quantities for the fluids in region 1 region 2 and region 3

References

[1]. Nel, A.E., Madler, L., Velegol, D., Xia, T., Hoek, E.M.V., Somasundaran, P., Klaessig, F., Castranova, V., Thompson, M., "Understanding biophysicochemical interactions at the nano-bio interface", *Nature Materials J.* 8, 543-557, (2009).

[2]. Davis, M.E., Chen, Z., Shin, D.M., "Nanoparticle therapeutics: an emerging treatment modality for cancer", *Nature Reviews Drug Discovery*, 7, 771-782, (2008).

[3]. Ozturk, S., Hassan, A.Y., Ugaz, V.M., "Interfacial complexation explains anomalous diffusion in nanofluids", *Nano Letters*, 10, 665-671, (2010).

[4]. Choi, S.U.S., " Nanofluids: from vision to reality through research", *ASME J. Heat Transfer*, 131, 1-9, (2009).

[5]. Keblinski, P., Eastman, J.A., Cahill, D.G., *Nanofluid for thermal transport, Mater.Today* 8 (2005), 36-44.

[6]. Wang, X.Q., Mujumdar, A.S., "Heat transfer characteristics of nanofluids": a review, *Int. J. Therm. Sci.*, 46, 1-19 (2007).

[7]. Mohammed, H.A., Al-aswadi, A.A., Shuaib, N.H., Saidur, R., "Convective heat transfer and fluid flow study over a step using nanofluids", *Renew. Sustain. Energy Rev.* 15, 2921-2939, (2011).

[8]. Xuan, Y. and Li, Q. "Heat transfer enhancement of nanofluids", *Int. J. Heat Fluid Flow*, **21**, 58–64, (2000)

[9]. Eastman, J. A., Choi, S. U. S., Li, S., Yu,W., Thompson, L. J. "Anomalously increased effective thermal conductivities of ethylene glycol-based nanofluids containing copper nanoparticles", *Appl. Phys. Lett.*, **78**, 718–720, (2001).

[10]. Xie, H., Wang, J., Xi, T. G., Liu, Y., Ai, F. "Thermal conductivity enhancement of suspensions containing nanosized alumina particles". *J. Appl. Phys.*, **91**, 4568–4572, (2002).

[11]. Hong, T. K., Yang, H. S., Choi, C. J. "Study of the enhanced thermal conductivity of nanofluids". *J. Appl. Phys.*, **97**, 1–4 (2005).

[12]. Daungthongsuk, W., Wongwises, S. "A critical review of convective heat transfer of nanofluids". *Renewable Sustainable Energy Reviews*, **11**, 797–817, (2007).

[13]. Zhou, D. W. "Heat transfer enhancement of copper nanofluid with acoustic cavitation". *Int. J. Heat Mass Transfer*, **47**, 3109–3117, (2004).

[14]. Choi, S. "Enhancing thermal conductivity of fluids with nanoparticle. *Developments and Applications of Non-Newtonian Flows* (eds. Siyiner, D. A. and Wang, H. P.), San Francisco, United States, **66**, 99–105, (1995).

[15]. Xuan, Y. and Li, Q. "Investigation on convective heat transfer and flow features of nanofluids". *Journal of Heat Transfer*, **125**, 151–155, (2003).

[16]. Shenoy, A.V., "Non-Newtonain Fluid Heat Transfer in Porous Media", *Adv. Heat Transfer* 24, 101-190, (1994).

[17]. Buongiorno, J., "Convective Transport in Nanofluids", *ASME J. Heat Transf.* 128, 240-250, (2006).

[18]. Das, S.K., Choi, S.U.S., Yu, W., Pradeep, T., Nanofluids: Science and Technology (Wiley, New Jersey, 2007).

[19]. Kakac¸ S., Pramuanjaroenkij, C. A., "Review of convective heat transfer enhancement with nanofluids", *Int. J. Heat Mass Transf.* 52, 3187-3196, (2009).

[20]. Jaluria, Y., Manca, O., Poulikakos, D., Vafai, K., Wang, L., "Heat transfer in nanofluids",*Adv. Mech. Eng.* 4, 972-993, (2012).

[21]. Mahian, O., Kianifar, A., Kalogirou, S.A., Pop, I., Wongwises, S.*,"A review of the applications of nanofluids in solar energy", Int. J. Heat Mass Transf.* 57, 582-594, (2013).

[22]. Sakai, F., Li, W., Nakayama, A., "A rigorous derivation and its applications of volume averaged transport equations for heat transfer in nanofluids saturated metal foam", in *Proceedings of 15th International Heat Transfer Conference, IHTC*-15, August 10-15, Kyoto, Japan, (IHTC, 2015) doi: 10.1615/IHTC15.pmd.008575.

[23]. Umavathi, J.C., Monica B Mohite, "The onset of convection in a nanofluid saturated porous layer using Darcy model with cross diffusion", *Meccanica*, vol. 49, pp. 1159-1175, (2014).

[24]. Umavathi, J.C., Monica B Mohite, " Double diffusive convective transport in a nanofluid-saturated porous layer with cross diffusion and variation of viscosity and conductivity", *Heat Tansfer Asian Research* , .43, 628-652, (2014).

[25]. Umavathi, J.C., Monika B Mohite, "Convective transport in aporous medium layer saturated with a Maxwell Nanofluid", *j. King Saud University, Engngn. Sciences*, 44, 227-256, (2015).

[26]. Umavathi, J. C., Ali Chamkha and Monika B Mohite, " Convective transport in a nanofluid-saturated porous layer with cross diffusion and variation of viscosity and conductivity", *Special Topics and Reviews in porous Medium*, 6, 1-17, (2015).

[27]. Umavathi J.C., "Rayleigh-Benard convection subject to time dependent wall temperature in a porous medium layer saturated by a nanofluid*", Meccanica,* 50, 981-994, (2015).

[28]. Umavathi, J.C., Sheremet, M.A., Odelu Ojjela, Janardhan Reddy, G., "The onset of double- diffusive convection in a nanofluid saturated porous layer: Cross- diffusion effects" *European journal of Mechanics*, 65, 70-87, (2017).

[29]. Umavathi , J.C., Mikhail A. Shermet, " Onset of double-diffusive convection of a sparsely packed micropolar fluid in a porous medium layer saturated with a nanofluid", *Microfluidic Nanofluid*, 21, 121-128, (2017).

[30]. Umavathi, J.C., Pratap Kumar, J., " Onset Convection in a porous medium layer saturated with an Oldroyd Nanofluid", *ASME J. of Heat Transfer*, vol. 139, 012401, 1-14, 2017.

[31]. Umavathi, J.C., Shermet, M.A., "Influence of temperature dependent conductivity of a nanofluid in a vertical rectangular duct" *Int. J. Nonlinear Mechanics*, 78, 17-28 , (2016).

[32]. Umavathi, J.C., "Heat transfer in avertical rectangular duct filled with a nanofluid for variable viscosity", *J. Nanofluid*, 6, 1-9, (2017).

[33]. Schwabe, D.,surface-tension-driven flow in crystal growth metals, *Crystal*, 11, 848-852, (1986).

[34]. Alazmi, B., Vafai, K.," Analysis of fluid flow and heat transfer interfacial conditions between a porous medium and a fluid Layer", *International Journal of Heat and Mass Transfer*, 44, 1735-1749, (2001).

[35]. Vafai, K., Thiyagaraja , R., "Analysis of Flow and Heat transfer at the interface region of a porous medium", *Int. J . Heat Mass Transfer* 30, 1987, pp. 1391-1405.

[36]. Umavathi, J.C., Chamka, A.J. , Abdul Mateen, Ai-Mudaf , A. ," Unsteady two fluid flow and heat transfer in ahorizontal channel", *Heat Mass Transfer*, 42, 81-90, (2005).

[37]. Malshetty, M.S., Umavathi, J.C., Prathap Kumar, J.," Magnetoconvection of two immiscible fluids in a vertical enclosure", *Heat Mass Transfer*, 42, 977-903, (2006).

[38]. Umavathi, J.C., Pratap Kumar, J., Chamka, A.J., " Flow and heat transfer of a micropolar fluid sandwiched between viscous fluid layers", *Canadian J. Physics*, 86, 961-973, (2008).

[39]. Pratap Kumar, J., Umavathi, J.C., Chamkha, A.J., Pop, I.," Fully developed free convective flow of micropolar and viscous fluid in a vertical channel", *Appl. Mathematical Modeling*, 34, 1175-1186, (2010).

[40]. Umavathi, J.C., Ali. Chamkha J., Sridhar, K.S.R., "Generalised plain Coutte flow heat transfer in a composite channel" , *Trans Porous Media*, 85, 157-169, (2010).

[41]. Umavathi, J.C., Liu, I.C., Pratap Kumar, J., "Magnetohydrodynamic Poiseuille-Coute flow and heat transfer in an inclined channel", *J. Mechanics*, 26, 525-532, (2010).
[42]. Liu, I.C., Umavathi, J.C., Wang, H-H., "Poiseuille-Coutte flow and heat transfer in an inclined composite porous medium", *J. Mech.*, 28, 559-56, (2012) .
[43]. Brinkman, H.C., "The Viscosity of concentrated suspensions and solutions", *J. Chem. Phys.*, 20, 1952**,** 571
[44]. Maxwell, J., 2nd ed. *Oxford University Press, Cambridge, UK*, (1904).
[45]. Vajravelu, K., Prasad, K.V., Abbasandy, S.," Convective transport of nanoparticles in multi-layer fluid flow", Appl. Math. Mech. –Engl. Ed., 343, 177-183, (2013) .
[46]. Tiwari, R.K., Das, M.K. , "Heat transfer augmentation in a two-sided lid-driven differentially heated square cavity utilizing nanofluids", *Int. J. Heat and Mass Transfer*, 50, 2002-2018, (2007).
[47]. Umavthi, J.C., Shekhar, M., "Effect of MHD on Jeffery-Hamel Flow in Nanofluids by Differential Transform Method", *Int. J. Eng. Res. Appl.*, 3, 953-962 (2013).
[48]. Shekhar, M., Umavathi, J.C.,"Influence of Viscous Dissipation on non-Darcy Mixed Convection Flow of Nanofluids", *HTAR*, 46, 176-199, (2017) .
[49] Umavathi, J.C., Odelu Ojjela, K. Vajravelu, "Numerical analysis of Natural Convective flow and heat transfer of nanofluids in a vertical rectangular duct using Darcy-Forchheimer Brinkman model", *IJTS*, 111, 511-524 (2017).